The effects of Bone marrow mesenchymal stem cells on m6A RNA methylation modification profile of aged granulosa cells

Chuan Tian
Kunming General Hospital of the People's Liberation Army: People's Liberation Army Joint Logistic Support Force 920th Hospital

Yuanyuan An
Kunming Medical University Affiliated Stomatology Hospital

Xiangqing Zhu
Kunming General Hospital of the People's Liberation Army: People's Liberation Army Joint Logistic Support Force 920th Hospital

Wei Wei
Kunming General Hospital of the People's Liberation Army: People's Liberation Army Joint Logistic Support Force 920th Hospital

Guangping Ruan
Kunming General Hospital of the People's Liberation Army: People's Liberation Army Joint Logistic Support Force 920th Hospital

Jing Zhao
Kunming General Hospital of the People's Liberation Army: People's Liberation Army Joint Logistic Support Force 920th Hospital

Ye Li
Kunming General Hospital of the People's Liberation Army: People's Liberation Army Joint Logistic Support Force 920th Hospital

xinghua pan (xinghuapankm@163.com)
Kunming General Hospital of the People's Liberation Army: People's Liberation Army Joint Logistic Support Force 920th Hospital

---

Research Article

Keywords: BMMSCs, ovarian ageing, m6A, KDM8, granulosa cell ageing

Posted Date: April 18th, 2022

DOI: https://doi.org/10.21203/rs.3.rs-1530027/v1

Abstract

Background

Ovarian ageing causing endocrine disturbances and degenerates systemic tissue and organ functions, seriously affects women's physical and mental health, effective treatment methods are urgently needed. On the basis of our previous studies on juvenile rhesus monkey bone marrow mesenchymal stem cells(BMMSCs) treated ovarian ageing of rhesus monkey, found that BMMSCs improved the ovarian structure and function. This study continues to explore the mechanism of BMMSCs reversd granulosa cell(GC) ageing.

Methods

Established GC ageing model and coculture system of BMMSCs, detected m6A methylation modification changes, performed m6A modified RNA immunoprecipitation sequencing (MeRIP-seq), corrected between m6A peaks with mRNA expression, and identified the expression of hub genes through q-PCR, Immunofluorescence staining, and western blot .

Results

Our results showed that H_2O_2 induced GC aging successfully and that BMMSCs reversed measures of GC ageing, BMMSCs promoted the expression of FTO and reduced the overall methylation level of m6A. We identified 797 m6A peaks (348 hypomethylated, 449 hypermethylated) and 817 differentially expressed genes (DEGs) (412 upregulated, 405 downregulated) after aged GCs cocultured with BMMSCs, which associated with ovarian function and epigenetic modification. Lysine Demethylase 8 (KDM8) involve in the negative regulation of osteoblast differentiation which was contracted with the positive regulation of osteoblast differentiation to mediate cellular senescence, and downregulated after treated with BMMSCs.

Conclusions

KDM8 may become new target in BMMSCs reversed ovarian ageing.

Introduction

The world's population is ageing rapidly, and the number of elderly individuals has increased significantly, which has placed great pressure on society and become one of the major economic challenges facing contemporary society[1–3]. The ovary is a dynamic reproductive endocrine organ that enacts female reproductive function through ovulation and the secretion of sex hormones and affects tissues and organs of the whole body[4, 5], which is one of the most sensitive organs to ageing. A variety of stimuli can lead to ovarian ageing, which makes women infertile and can be accompanied by related growth and

developmental diseases, these are serious threats to women's health[6–8]. At the molecular level, ovarian ageing is gradual and involves multifactor interactions and complex biological processes; it is caused by decreases in follicle quantity and quality and is related to autoimmunity, genetic susceptibility, mitochondria, and telomerase[9–11]. However, the mechanisms of transcription, regulation and modification of reproductive helper cells in the occurrence and development of ovarian ageing are not clear, which hinders the progress of effective treatment of ovarian ageing.

The ageing ovary is mainly characterized by tissue structure atrophy, lack of self-renewal ability of reproductive helper cells, decreased cell numbers and functional degeneration. Bone marrow mesenchymal stem cells (BMMSCs) have several biological characteristics: multidirectional differentiation potential, strong self-renewal ability, and the ability to secrete multiple cytokines and repair tissue[12, 13]. As such, they may become a novel tool for reversing ovarian ageing. Many studies have shown that mesenchymal stem cells (MSCs) are safe and effective in the treatment of ovarian ageing, and they are a more effective cell type to improve ovarian structure and function[14]. Previous studies have confirmed that MSCs can regulate women's sex hormone secretion, promote follicular regeneration, and restore the activity and number of reproductive helper cells[15–18]. However, the transcriptional modification profile and key regulatory signalling pathways of MSCs in the treatment of ovarian ageing are not clear, and systematic research with comparisons to normal controls is lacking.

N6-methyladenosine (m6A) is a common internal modification of mRNA and has many effects on the fate of mRNA[19]. Recent studies have found that m6A plays an important role in regulating gene expression, splicing, RNA editing, and RNA stability, controlling mRNA lifespan and degradation, and mediating circular RNA translation[20, 21]. In addition, previous studies have showed that m6A was significantly associated with ovarian ageing and ageing-related diseases[22–25]. However, whether BMMSCs affect ovarian ageing by regulating m6A modification of RNA methylation has not yet been fully investigated,which attracted our attention.

Therefore, for exploring the mechanism by which MSCs participate in ovarian ageing, human granulosa cell (hGC) ageing model was established and were cocultured with BMMSCs in vitro. MeRIP-seq and bioinformatics Analysis were used to explore the overall effect of BMMSCs on m6A RNA methylation modification with mRNA expression profiles, and identify the key factor and regulatory signalling pathways through a variety of biotechnologies, to provide theoretical basis for the use of MSCs in treating ovarian ageing.

Results

H_2O_2-induced hGC ageing, and cocultured with BMMSCs.

hGCs are the most important cells in the ovary, therefore, an hGC ageing model was established in vitro to further explore the mechanism of BMMSCs in ovarian ageing. As a small molecule oxidant, H_2O_2 can easily cause cell ageing by inducing oxidative stress through the biofilm system, and this technique has

been widely applied to induce cell ageing[28, 29]. In our study, hGCs were exposed to H_2O_2 for 24 h and cocultured with BMMSCs for 48 h. First, β-galactosidase staining (blue staining with β-galactosidase activity) (Figure 1A) showed that 7.33±1.69% of the hGCs stained blue in the control group, 93.33±0.47% in the model group, and 43.66±2.05% in the coculture group (Figure 1B). Proliferation and division reflect the activation of hGCs. BrdU staining (red) showed that hGCs were proliferating and dividing (Figure 1C): 87.66±1.24% of hGCs were stained red in the control group, 16.33±1.24% in the model group, and 80.66±1.24% in the coculture group (Figure 1D) . Finally, reactive oxygen species (ROS) are an important ageing marker[30, 31], and DEH staining showed that the level of ROS was 3.77±0.12% in the control group, 8.63±0.12% in the model group, and 5.63±0.12% in the coculture group (Figures 1E,F), Next, immunohistochemical staining was performed to detect the expression of P53 protein (Figure 1G), and the results showed that 21.04±0.48% of cells expressed P53 protein in the control group, 58.20±1.21% in the model group, and 42.90±1.41% in the coculture group (Figure 1H),which suggested that the hGCs were ageing after 273 mM H_2O_2 treatment for 24 h, and BMMSCs recovered these ageing markers in aged hGCs.

The changes of m6A RNA methylation modificationin in aged hGCs and after BMMSCs treated

Studies have proved that the expression of demethylase FTO was down-regulated in ovarian tissue with the increase of age to promote ovarian aging[26, 27]. However, it whether BMMSCs could regulate FTO to effect methylation modification remains unclear, Interestingly, our results showed that compared with the model group, the expression of FTO was up-regulated after BMMSCs treatment in vivo (Figure 2A, B), and also significantly up-regulated after aged hGCs were co-cultured with BMMSCs in vitro (Figure 2C, D, E, F). In addition, the overall level of m6A was significantly decreased after co-cultured with BMMSCs (Figure 2G), which suggested that hGC ageing is closely related to m6A methylation modification, and BMMSCs play an key role in regulating m6A methylation modification.

Overview of the m6A methylation landscape in aged hGCs and after cocultured with BMMSCs.

m6A is the most prevalent RNA modification of mRNAs and lncRNAs and plays a key role in ageing and various ageing diseases[32, 33]. However, its specific regulatory mechanism in ovarian ageing remains unclear. In our study, after induced hGCs ageing and cocultured with BMMSCs, MeRIP-seq were performed to explore the effect of BMMSCs on m6A modification of hGC ageing. Our results showed that 7,923 transcripts displayed a total of 14,417 sites that were modified by m6A in the model group, and 6,867 transcripts displayed a total of 11,715 sites that were modified by m6A in the coculture group. Among them, 14,241 individual m6A peaks in 9,741 m6A-modified genes were detected in the model and coculture groups (Figure 3A). Notably, the coculture group had 6,109 new peaks and 9,088 missing peaks compared to the model group, revealing that the global m6A modification patterns were markedly different between the model and coculture groups (Figure 3B). As shown in Figure 3C, D, the results showed different patterns of peaks with a relative increase in the start codon region (6.4 vs. 5.7% for aged hGCs and aged hGCs cocultured with BMMSCs, respectively) and in the 3’ untranslated region (3’UTR, 39.4 vs. 37.6%) and a relative decrease in the coding sequence (CDS, 30 vs. 32.3%) and at the stop codon

(20.1 vs. 21%). Figure 3E shows that the distribution of m6A signals around mRNAs and lncRNAs was comparable in the model and coculture groups. In general, m6A peaks tended to occur in CDS regions and 3'UTR, which means that m6A is likely to play a crucial role in regulating mRNA expression and affecting the stability of the mRNA, consistent with previous MeRIP-seq results[34, 35]. The m6A peak distribution analysis suggested that most mRNAs and genes had m6A peaks, and there were mostly 1 to 3 m6A modifications in the exons (Figures 3F, G, H). In addition, m6A peaks were found in all chromosomes, with the highest numbers being in chr1, chr17, and chr19 (Figures 3I).

Differentially m6A peaks in model and cocolture group

To explore the biological significance of m6A modification in BMMSCs interacting with aged hGCs, GO and KEGG pathway analyses of differentially methylated mRNAs were conducted. As shown in Figure 4A, compared to aged hGCs, after cocultured with BMMSCs had 449 significantly upregulated m6A peaks and 348 downregulated m6A peaks (fold changes≥2). Furthermore, the classic GGACU motif and the top 5 m6A motifs were observed in the model (Figure 4B) and coculture groups (Figure 4C). GO process results showed that the altered m6a peaks were significantly enriched in chromatin modification, regulation of transcription, DNA–templated, and cell cycle (Figure 4D). Additionally, in KEGG pathway analyses, the Spliceosome, Epstei-Barr virus infection, and Thyroid hormone signaling pathway were signifificantly correlated with genes that showed m6A peaks in aged hGCs (Figure 4E). It can been said that m6A peaks were play a key role in ovarian ageing.

Changes in mRNA in aged hGCs and after cocultured with BMMSCs

First, we tested the transcriptome profiles of altered genes in three pairs of aged hGCs and aged hGCs after cocultured with BMMSCs using MeRIP-seq. Compared to aged hGCs, hGCs cocultured with BMMSCs had 412 significantly upregulated genes and 405 significantly downregulated genes (|log2FC| > 1, P value < 0.05) (Figure 5A), which PPI networks are presented in Figure 5B and 5C. Functional network analysis showed that the 412 genes were involved in regulation of mitotic sister chromatid segregation, positive regulation of protein localization to endosomes, and cellular senescence (Figure 5D). The KEGG pathway analysis mainly identified enrichment of the terms cytokine-cytokine receptor, pentose phosphate pathway, rheumatoid athritis, and TNF signaling pathway(Figure 5F). In addition, the 405 genes were found to be involved in purine nucleoside triphosphate biosynthetic processes, neural crest cell migration, and embryonic camera-type eye formation(Figure 5E), and were significantly enriched in the terms nonhomologous end-joining, the Hippo signalling pathway, sphingolipid metabolism, and the homologous recombination signalling pathway (Figure 5G).

Correlation between differential m6A peaks and differential expression of mRNA

Correlation analyses of altered m6A peaks with differentially expressed mRNAs (|log2FC| > 1, P value < 0.05) were performed to identify the key genes through which BMMSCs affect m6A methylation modification of hGCs during ageing (Figure 6A, B). The cumulative differential mRNA abundance is shown in Figure 6C. We identified 42 hypermethylated m6A peaks in mRNAs that were significantly

upregulated (3) or downregulated (39), while 88 hypomethylated m6A peaks in mRNAs were significantly upregulated (74) or downregulated (14) (Figure 6D). Next, 130 genes that showed significant changes in both m6A modification and RNA expression levels were subjected to GO, pathway and PPI network analyses. The GO analyses of processes associated with the 130 gene sets are shown in detail in Figure 6E and identified numerous linked functional processes and pathways. Interestingly, we found that the top 3 GO terms of histone H3-K36 demethylation (KDM8 and RIOX1), regulation of apoptotic DNA fragmentation, and regulation of DNA catabolic process were enriched in the GO maps of aged hGCs cocultured with BMMSCs (Figure 6E). Interestingly, the correlation of histone H3-K36 demethylation was consistent with the results of the DEG GO analysis (Figure 5E). In addition, the top 20 KEGG pathways that are shown in Figure 6F, which were significantly enriched in metabolism, genetic information processing, and environmental information processing. Moreover, the EcCenticity analysis results showed that KDM8 ranks first in the PPI network (Figure 6G), and involved in negative regulation of osteoblast differentiation and circadian regulation of gene expression (Figures 6H). KDM8 m6A peak visualization by IGV is shown in Figure 6I. These observations indicate that KDM8 with m6A modification may play important roles in the reversal of hGC ageing induced by BMMSCs.

The expression of KDM8 in aged GCs before and after cocultured with BMMSCs

KDM8 (Lysine Demethylase 8) as the epigenetic repressive mark and important cell cycle regulator, which functioned as a transcriptional activator by inhibiting HDAC recruitment via demethylation of H3K36me2[36], and involve in osteoblast differentiation[37]. Methylation modifications of histones play critical roles in regulating gene expression, cell cycle, genome stability, and nuclear structure, therefore, we explored the regularity of KDM8 in hGCs and ovarian tissue, and the intervening effect of BMMSCs. Our results showed that compared with the elderly model group, the expression of KDM8 was down-regulated after BMMSCs treatment in macaques(Figure 7A, B), and also down-regulated after co-cultured with BMMSCs in vitro(Figure 7C,D,E), while histone of H3 was up-regulated in hGCs after cocultured with BMMSCs(Figure 7F).

Discussion

BMMSCs with multidirectional differentiation potential, strong self-renewal ability, combating oxidative stress and inflammation, secreting various cytokines, which have been postulated to play a key role in reversing ovarian ageing, moreover, hGCs are the most important auxiliary cells which provide support and nutrition for follicles and oocytes[38], therefore, we used BMMSCs treated with aged hGCs in a Transwell system to explore the interaction mechanism. Interestingly, our results showed that the structure and function of ovary significantly improved after BMMSCs treatment, the levels of β-galactosidase and ROS increased, proliferation was weakened, and the expression of p53 protein was upregulated, which demonstrated that the hGCs were ageing. After aged hGCs were cocultured with BMMSCs, the above factors related to ageing recovered to normal levels comparable with those of the model group, demonstrating that a model of ageing hGCs was successfully established and that BMMSCs could reverse hGCs ageing.

m6A has been reported as a novel factor in epigenetic modification that is strongly associated with ageing and various ageing diseases[39, 40]. However, whether BMMSCs can reverse hGCs ageing through m6A modification remains unclear. In our study, Compared to control group, the expression of FTO downregulated and the overall m6A levels increased in the model group, which were consist with previous study that increased m6A in hGCs can mediate faster aging-related phenotypes resulting in ovarian ageing[41], while the expression of FTO upregulated and the overall m6A levels decreased after BMMSCs treatment. In addition, We found 797 altered m6A peaks after BMMSCs treatment, and they were significantly enriched in chromatin modification, regulation of transcription, DNA-templated, and cell cycle, which were associated with ovarian ageing. Additionally, in KEGG pathway analyses, the Spliceosome, Epstein-Barr virus infection, and Thyroid hormone signaling pathway were signifificantly correlated with genes that showed m6A peaks in aged hGCs, which suggested that m6A methylated modification peaks play a key role in regulating ovarian ageing.

In the mRNA transcriptional profile analysis, we found that a total of 817 genes changed after aged hGCs cocultured with BMMSCs, which 412 genes upregulated and 405 genes downregulated. The 412 genes were found to have functions involved in the regulation of mitotic sister chromatid segregation, positive regulation of protein localization to endosomes, and cellular senescence, and the 405 genes significantly associated with embryonic placenta morphogenesis and fertilization, which have been linked to epigenetic modification and female fertilization function. These results suggested that BMMSCs interact with aged hGCs may through regulating those mRNA transcriptional profile to reverse ovarian ageing.

By combining MeRIP-seq and RNA-seq data, we identified 42 hypermethylated m6A peaks in mRNAs that were significantly upregulated (3) or downregulated (39) and 88 hypomethylated m6A peaks in mRNAs that were significantly upregulated (74) or downregulated (14). we found that histone H3-K36 demethylation (KDM8 and RIOX1) rank first in the GO analysis, and the enriched pathways mainly included metabolism, genetic information processing, and environmental information processing. Interestingly, the correlation results regarding histone H3-K36 demethylation were consistent with the GO analysis of the DEGs, and the signaling pathway of KDM8 involved in negative regulation of osteoblast differentiation, which was contracted with cellular senescence is mediated through positive regulation of osteoblast differentiation, and coincides with the research findings that m6A was important to maintain the bone mass and functions to protect osteoblasts from the ROS-mediated cell ageing process[42]. KDM8 as the epigenetic repressive mark and important cell cycle regulator, at the same time, it's interesting that high expression of KDM8 can suppress migration and proliferation[43–45], which were consistent with our results that KDM8 was upregulated in the model group, while downregulated after BMMSCs treatment, therefore, KDM8 may be potential therapeutic targets in BMMSCs reversing hGC ageing.

In summary, BMMSCs recover hGC ageing-related indexes, upregulated the expression of FTO, decrease the overall level of m6A, and m6A methylation modification plays an important role in BMMSCs reversing hGC ageing. In the future, KDM8 may be novel target in BMMSCs to reverse hGC ageing.

Conclusion

i. BMMSCs significantly upregulated the expression of FTO, decreased overall levels of m6A RNA methylation modification.

ii. In the ageing model of hGCs, 273mM of H_2O_2 treated hGCs for 24 h, which lead to increased the levels of β-galactosidase and ROS, weakened proliferation, and upregulated the expression of p53 to induce hGCs ageing, while BMMSCs recovered above factors related to ageing.

iii. BMMSCs decreased overall levels of m6A in aged hGCs, m6A methylation modification mainly occurred in the CDS of mRNA to regulate their expression to induce or suppressed hGC ageing, and KDM8 may be novel target in BMMSCs to reverse hGC ageing.

Materials And Methods

Materials

BMMSCs were provided by the Basic Medical Laboratory of the 920th Hospital of Joint Logistics Support Force of PLA, The Transfer Medicine Key Laboratory of Cell Therapy Technology of Yunan Province, The Integrated Engineering Laboratory of Cell Biological Medicine of State and Regions. hGC were purchased from Bainer Chuanglian Biotechnology Co., Ltd.

Induction of hGCs ageing

When 80% hGC adherence was reached in 6-well plate, 273 mM H_2O_2 treated in model group for 24 h. β-Galactosidase staining was used to detect the expression of β-galactosidase[46], DHE staining was performed to detect the level of ROS [47], and BrdU staining were performed to observe the proliferation ability[48]. Immunohistochemical staining were used to detect the expression of p53 protein[49].

Aged hGCs cocultured with BMMSCs

A total of 10^4 hGCs were added to the lower chamber of the Transwell plate. When the confluence rate reached 80%, 273 mM H_2O_2 was treated for 24 h. Then the medium was changed, and 10^4 BMMSCs of P4 were added to the upper chamber of the Transwell plate for the model and coculture group, which cocultured for 48 h, and β-galactosidase staining, DHE staining, BrdU staining, and immunohistochemical staining were used to detect the relative ageing indexes.

Ccolorimetry

The overall methylation level detection kit (EpiQuik™ m6A RNA Methylation Quantification Kit, Colorimetric, Epigentek) can quantify m6A ribonucleic acid methylation, extract total RNA for m6A RNA capture, and then measure the signal on a 450 nm microplate reader detection.

MeRIP-seq

hGCs in the control, model, and coculture groups were collected, TRIzol was added to the lysate, and total RNA was extracted for reverse transcription. High-throughput sequencing was performed to obtain raw data, which were then extracted and quality controlled. Processing yielded clean reads, and FastQC was used to analyse the quality of sequencing data and obtain information. Mapping analyses identified the source of the sequencing sequence, its position in the genome, and unique mapped reads. HISAT2 software was used to compare the filtered clean reads with the reference genome of the corresponding species of the sample to obtain unique mapped reads for further analysis. The tdf file or bigwig file was converted from the processed bam file after standardization and used for IGV or Genome Browser (UCSC) visualization. ExomePeak was used to verify the quality of the data and the enrichment of short sequences in the genome. Peak annotation was analysed, and the gene structure and overall distribution characteristics of the peak were determined to draw metagene plots and pie diagrams. HOMER (http://homer.ucsd.edu/homer/ngs/peakMotifs.html) software was used to perform motif analysis of the peaks.

Differential peak analysis first identifies reads enriched in binding sites and then checks whether these sites have differential methylation modifications under the two experimental conditions and statistical tests. Differential m6A peak-modified genes were analysed with STRING and Cytoscape. The m6A-modified genes were analysed with GO and KEGG analyses, the logarithmic result of a significant P-value was used for visualization, and the first 20 terms were selected to draw a bubble chart.

Analysis of the correlation of m6A modifications with RNA expression

Genome version GRCh38_Ensembl91_year_2017 was used with htseq-count to count the number of reads in some units of the genome. Differential expression analysis was performed with DESeq2, and the significantly different gene criteria were as follows: 1. |log2FC|> 1; 2. P-value <0.05. Cluster analysis of the DEGs was performed. A normalized expression table of the selected differential genes was used as the input file. Fisher’s test was used to calculate the significance level (P-value) of each GO term and pathway. The m6A-modified genes and the mRNA expression level changes were analysed for correlation, and some key genes related to the ageing phenotype were identified for follow-up research. A cumulative distribution diagram and a four-quadrant diagram were generated to show the correlation analysis results.

Western blot

Collect the cells of each group, extract the total protein, use the BCA protein concentration assay kit to measure the protein concentration, add the protein solution to 5* reduced protein loading buffer in a ratio of 4:1, denature in a boiling water bath for 15 minutes, and perform SDS-PAGE electrophoresis , transfer the membrane with 300mA constant current, block the transferred membrane with skim milk for 30min, add primary antibody (FTO, KDM8) and incubate at 4°C overnight, wash the membrane three times with

TBST, 5min each time. The secondary antibody was added and incubated for 30 min, and the membrane was washed three times with TBST for 5 min each time for development and fixation.

Abbreviations

Abbreviations	Full name
BMMSCs	Bone marrow mesenchymal stem cells
hGC	human granulosa cell
MeRIP-seq	m6A-modified RNA immunoprecipitation sequencing
KDM8	Lysine Demethylase 8
m6A	N6-methyladenosine
DEGs	differentially expressed genes

Declarations

Ethical approval and consent to participate

Animal production licence number: SCXK (Dian) K2017-0003. The use of macaques was approved by the experimental animal ethics committee of the relying unit, and the approval number was Lengshen 2019-032 (Section)-01 with the animal licence number SYXK (Military) 2012-0039.

Consent for publication

Not applicable.

Availability of data and material

All data generated or analysed during this study are included in this published article.

Competing interests

The authors declare that they have no competing interests.

Funding

This work was supported by grants from the Yunnan Science and Technology Plan Project Major Science and Technology Project (2018ZF007) and the project en titled Transformation of subtotipotent stem cells based on the tree shrew model of multiple organ dysfunction syndrome SYDW[2020]19.

Authors' contributions

XHP designed the research, CT, YYA, XQZ, WW, JZ and YL performed the experiments, CT collected the data and wrote the manuscript. YYA and GPR assisted with the literature searches and revised the manuscript. All authors read and approved the final manuscript.

Acknowledgements

We thank everyone on our team for assisting with the preparation of this manuscript.

References

1. Barrera-Vazquez OS, Gomez-Verjan JC. The Unexplored World of Human Virome, Mycobiome, and Archaeome in Aging. J Gerontol A Biol Sci Med Sci. 2020;75:1834–7.
2. Grande G, Qiu C, Fratiglioni L. Prevention of dementia in an ageing world: Evidence and biological rationale. Ageing Res Rev. 2020;64:101045.
3. Khosla S, Farr JN, Tchkonia T, Kirkland JL. The role of cellular senescence in ageing and endocrine disease. Nat Rev Endocrinol. 2020;16:263–75.
4. Moolhuijsen L, Visser JA. Anti-Mullerian Hormone and Ovarian Reserve: Update on Assessing Ovarian Function. J Clin Endocrinol Metab. 2020;105.
5. Fan X, Bialecka M, Moustakas I, Lam E, Torrens-Juaneda V, Borggreven NV, et al. Single-cell reconstruction of follicular remodeling in the human adult ovary. Nat Commun. 2019;10:3164.
6. Park SU, Walsh L, Berkowitz KM. Mechanisms of ovarian aging. Reproduction. 2021;162:R19–33.
7. Li CJ, Lin LT, Tsai HW, Chern CU, Wen ZH, Wang PH, et al. The Molecular Regulation in the Pathophysiology in Ovarian Aging. Aging Dis. 2021;12:934–49.
8. Helvaci N, Yildiz BO. Cardiovascular health and menopause in aging women with polycystic ovary syndrome. Expert Rev Endocrinol Metab. 2020;15:29–39.
9. Tesarik J, Galan-Lazaro M, Mendoza-Tesarik R. Ovarian Aging: Molecular Mechanisms and Medical Management. Int J Mol Sci. 2021;22.
10. Yang L, Chen Y, Liu Y, Xing Y, Miao C, Zhao Y, et al. The Role of Oxidative Stress and Natural Antioxidants in Ovarian Aging. Front Pharmacol. 2020;11:617843.
11. Busnelli A, Navarra A, Levi-Setti PE. Qualitative and Quantitative Ovarian and Peripheral Blood Mitochondrial DNA (mtDNA) Alterations: Mechanisms and Implications for Female Fertility. Antioxidants (Basel). 2021;10.
12. Arthur A, Gronthos S. Clinical Application of Bone Marrow Mesenchymal Stem/Stromal Cells to Repair Skeletal Tissue. Int J Mol Sci. 2020;21.
13. Hernigou P, Delambre J, Quiennec S, Poignard A. Human bone marrow mesenchymal stem cell injection in subchondral lesions of knee osteoarthritis: a prospective randomized study versus contralateral arthroplasty at a mean fifteen year follow-up. Int Orthop. 2021;45:365–73.
14. Kim KH, Kim EY, Kim GJ, Ko JJ, Cha KY, Koong MK, et al. Human placenta-derived mesenchymal stem cells stimulate ovarian function via miR-145 and bone morphogenetic protein signaling in aged

rats. Stem Cell Res Ther. 2020;11:472.

15. Fabregues F, Ferreri J, Mendez M, Calafell JM, Otero J, Farre R. In Vitro Follicular Activation and Stem Cell Therapy as a Novel Treatment Strategies in Diminished Ovarian Reserve and Primary Ovarian Insufficiency. Front Endocrinol (Lausanne). 2020;11:617704.
16. El-Derany MO, Said RS, El-Demerdash E. Bone Marrow-Derived Mesenchymal Stem Cells Reverse Radiotherapy-Induced Premature Ovarian Failure: Emphasis on Signal Integration of TGF-beta, Wnt/beta-Catenin and Hippo Pathways. Stem Cell Rev Rep. 2021;17:1429–45.
17. Buigues A, Marchante M, de Miguel-Gomez L, Martinez J, Cervello I, Pellicer A, et al. Stem cell-secreted factor therapy regenerates the ovarian niche and rescues follicles. Am J Obstet Gynecol. 2021;225:61–5.
18. Wang Z, Yang T, Liu S, Chen Y. Effects of bone marrow mesenchymal stem cells on ovarian and testicular function in aging Sprague-Dawley rats induced by D-galactose. Cell Cycle. 2020;19:2340–50.
19. Karthiya R, Khandelia P. m6A RNA Methylation: Ramifications for Gene Expression and Human Health. Mol Biotechnol. 2020;62:467–84.
20. Li Y, Gu J, Xu F, Zhu Q, Chen Y, Ge D, et al. Molecular characterization, biological function, tumor microenvironment association and clinical significance of m6A regulators in lung adenocarcinoma. Brief Bioinform. 2021;22.
21. Mapperley C, van de Lagemaat LN, Lawson H, Tavosanis A, Paris J, Campos J, et al. The mRNA m6A reader YTHDF2 suppresses proinflammatory pathways and sustains hematopoietic stem cell function. J Exp Med. 2021;218.
22. Jiang ZX, Wang YN, Li ZY, Dai ZH, He Y, Chu K, et al. The m6A mRNA demethylase FTO in granulosa cells retards FOS-dependent ovarian aging. Cell Death Dis. 2021;12:744.
23. Zhang S, Deng W, Liu Q, Wang P, Yang W, Ni W. Altered m(6) A modification is involved in up-regulated expression of FOXO3 in luteinized granulosa cells of non-obese polycystic ovary syndrome patients. J Cell Mol Med. 2020;24:11874–82.
24. Zhang J, Ao Y, Zhang Z, Mo Y, Peng L, Jiang Y, et al. Lamin A safeguards the m(6) A methylase METTL14 nuclear speckle reservoir to prevent cellular senescence. Aging Cell. 2020;19:e13215.
25. Trauner M, Gindin Y, Jiang Z, Chung C, Subramanian GM, Myers RP, et al. Methylation signatures in peripheral blood are associated with marked age acceleration and disease progression in patients with primary sclerosing cholangitis. JHEP Rep. 2020;2:100060.
26. Jiang ZX, Wang YN, Li ZY, Dai ZH, He Y, Chu K, et al. The m6A mRNA demethylase FTO in granulosa cells retards FOS-dependent ovarian aging. Cell Death Dis. 2021;12:744.
27. Jiang ZX, Wang YN, Li ZY, Dai ZH, He Y, Chu K, et al. Correction: The m6A mRNA demethylase FTO in granulosa cells retards FOS-dependent ovarian aging. Cell Death Dis. 2021;12:1114.
28. Yin Z, Park R, Choi BM. Isoparvifuran isolated from Dalbergia odorifera attenuates H2O2-induced senescence of BJ cells through SIRT1 activation and AKT/mTOR pathway inhibition. Biochem Biophys Res Commun. 2020;533:925–31.

29. Jiang F, Xu XR, Li WM, Xia K, Wang LF, Yang XC. Monotropein alleviates H2O2induced inflammation, oxidative stress and apoptosis via NFkappaB/AP1 signaling. Mol Med Rep. 2020;22:4828–36.
30. Quan Y, Xin Y, Tian G, Zhou J, Liu X. Mitochondrial ROS-Modulated mtDNA: A Potential Target for Cardiac Aging. Oxid Med Cell Longev. 2020;2020:9423593.
31. Madreiter-Sokolowski CT, Thomas C, Ristow M. Interrelation between ROS and Ca(2+) in aging and age-related diseases. Redox Biol. 2020;36:101678.
32. Qin L, Min S, Shu L, Pan H, Zhong J, Guo J, et al. Genetic analysis of N6-methyladenosine modification genes in Parkinson's disease. Neurobiol Aging. 2020;93:143–9.
33. Zhang J, Ao Y, Zhang Z, Mo Y, Peng L, Jiang Y, et al. Lamin A safeguards the m(6) A methylase METTL14 nuclear speckle reservoir to prevent cellular senescence. Aging Cell. 2020;19:e13215.
34. Sendinc E, Valle-Garcia D, Dhall A, Chen H, Henriques T, Navarrete-Perea J, et al. PCIF1 Catalyzes m6Am mRNA Methylation to Regulate Gene Expression. Mol Cell. 2019;75:620–30.
35. Liu J, Dou X, Chen C, Chen C, Liu C, Xu MM, et al. N (6)-methyladenosine of chromosome-associated regulatory RNA regulates chromatin state and transcription. Science. 2020;367:580–6.
36. Wilkins SE, Islam MS, Gannon JM, Markolovic S, Hopkinson RJ, Ge W, et al. JMJD5 is a human arginyl C-3 hydroxylase. Nat Commun. 2018;9:1180.
37. Munehira Y, Yang Z, Gozani O. Systematic Analysis of Known and Candidate Lysine Demethylases in the Regulation of Myoblast Differentiation. J Mol Biol. 2017;429:2055–65.
38. Ding Y, Zhu Q, He Y, Lu Y, Wang Y, Qi J, et al. Induction of autophagy by Beclin-1 in granulosa cells contributes to follicular progesterone elevation in ovarian endometriosis. Transl Res. 2021;227:15–29.
39. Shafik AM, Zhang F, Guo Z, Dai Q, Pajdzik K, Li Y, et al. N6-methyladenosine dynamics in neurodevelopment and aging, and its potential role in Alzheimer's disease. Genome Biol. 2021;22:17.
40. Chen X, Wang J, Tahir M, Zhang F, Ran Y, Liu Z, et al. Current insights into the implications of m6A RNA methylation and autophagy interaction in human diseases. Cell Biosci. 2021;11:147.
41. Jiang ZX, Wang YN, Li ZY, Dai ZH, He Y, Chu K, et al. The m6A mRNA demethylase FTO in granulosa cells retards FOS-dependent ovarian aging. Cell Death Dis. 2021;12:744.
42. Zhang Q, Riddle RC, Yang Q, Rosen CR, Guttridge DC, Dirckx N, et al. The RNA demethylase FTO is required for maintenance of bone mass and functions to protect osteoblasts from genotoxic damage. Proc Natl Acad Sci U S A. 2019;116:17980–9.
43. Yao Y, Zhou WY, He RX. Down-regulation of JMJD5 suppresses metastasis and induces apoptosis in oral squamous cell carcinoma by regulating p53/NF-kappaB pathway. Biomed Pharmacother. 2019;109:1994–2004.
44. Fuhrmann D, Mernberger M, Nist A, Stiewe T, Elsasser HP. Miz1 Controls Schwann Cell Proliferation via H3K36(me2) Demethylase Kdm8 to Prevent Peripheral Nerve Demyelination. J Neurosci. 2018;38:858–77.

45. Fuhrmann D, Elsasser HP. Schwann cell Myc-interacting zinc-finger protein 1 without pox virus and zinc finger: epigenetic implications in a peripheral neuropathy. Neural Regen Res. 2018;13:1534–7.
46. Truman AM, Tilly JL, Woods DC. Ovarian regeneration: The potential for stem cell contribution in the postnatal ovary to sustained endocrine function. Mol Cell Endocrinol. 2017;445:74–84.
47. Li W, Li Y, Zhao Y, Ren L. The protective effects of aloperine against ox-LDL-induced endothelial dysfunction and inflammation in HUVECs. Artif Cells Nanomed Biotechnol. 2020;48:107–15.
48. Ding C, Zou Q, Wang F, Wu H, Chen R, Lv J, et al. Human amniotic mesenchymal stem cells improve ovarian function in natural aging through secreting hepatocyte growth factor and epidermal growth factor. Stem Cell Res Ther. 2018;9:55.
49. Liu YA, Ji JX, Almadani N, Crawford RI, Gilks CB, Kinloch M, et al. Comparison of p53 immunohistochemical staining in differentiated vulvar intraepithelial neoplasia (dVIN) with that in inflammatory dermatoses and benign squamous lesions in the vulva. Histopathology. 2021;78:424–33.

Figures

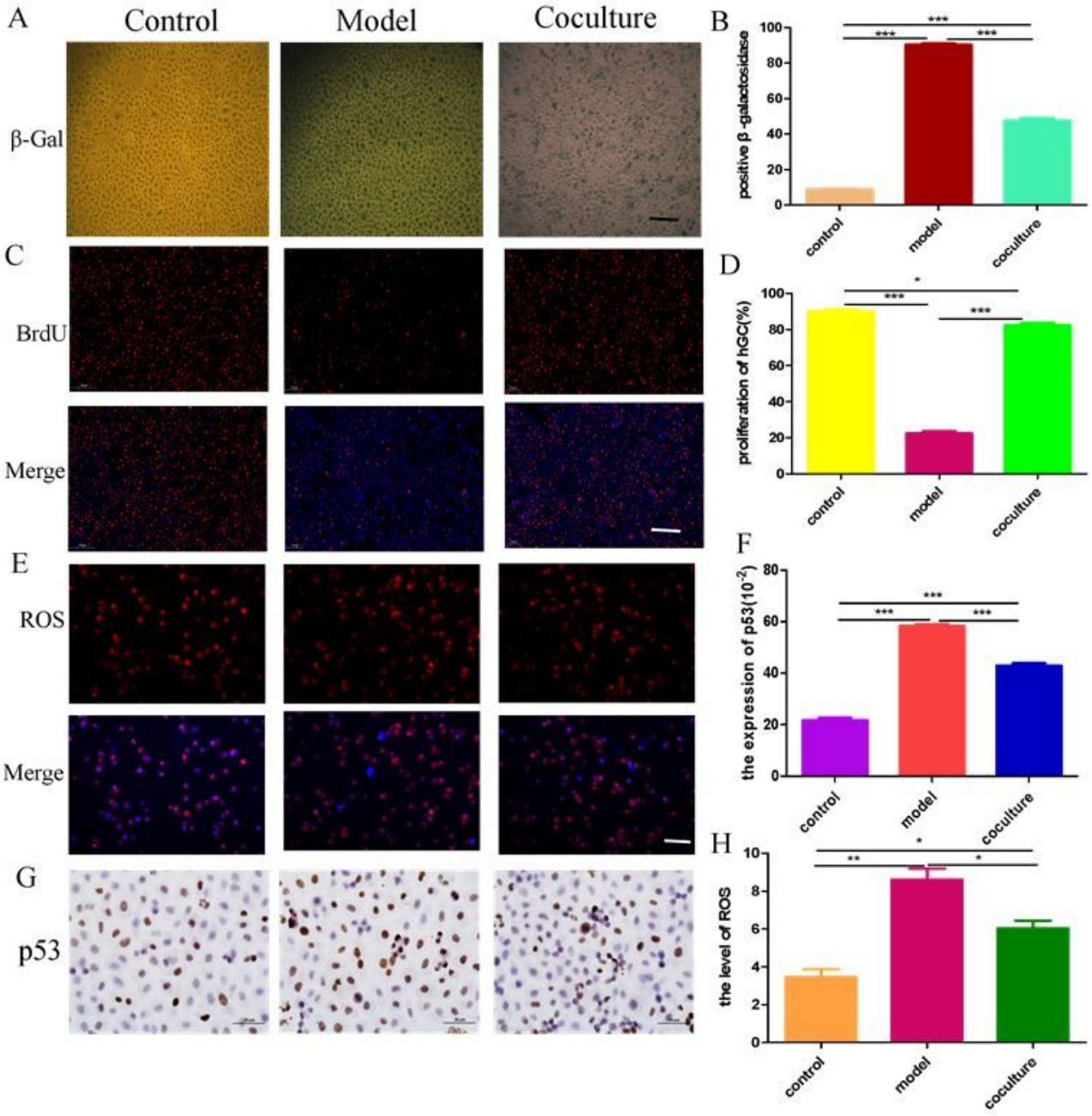

Figure 1

hGC ageing model and cocultured with BMMSCs. **A-B** β-Galactosidase staining detected the activity of β-galactosidase (100×). **C-D** BrdU staining observe hGC proliferation and division (100×). **E-F** DEH staining detected the level of ROS (200×). G-H Immunohistochemical staining detected the expression of p53(50 μm).

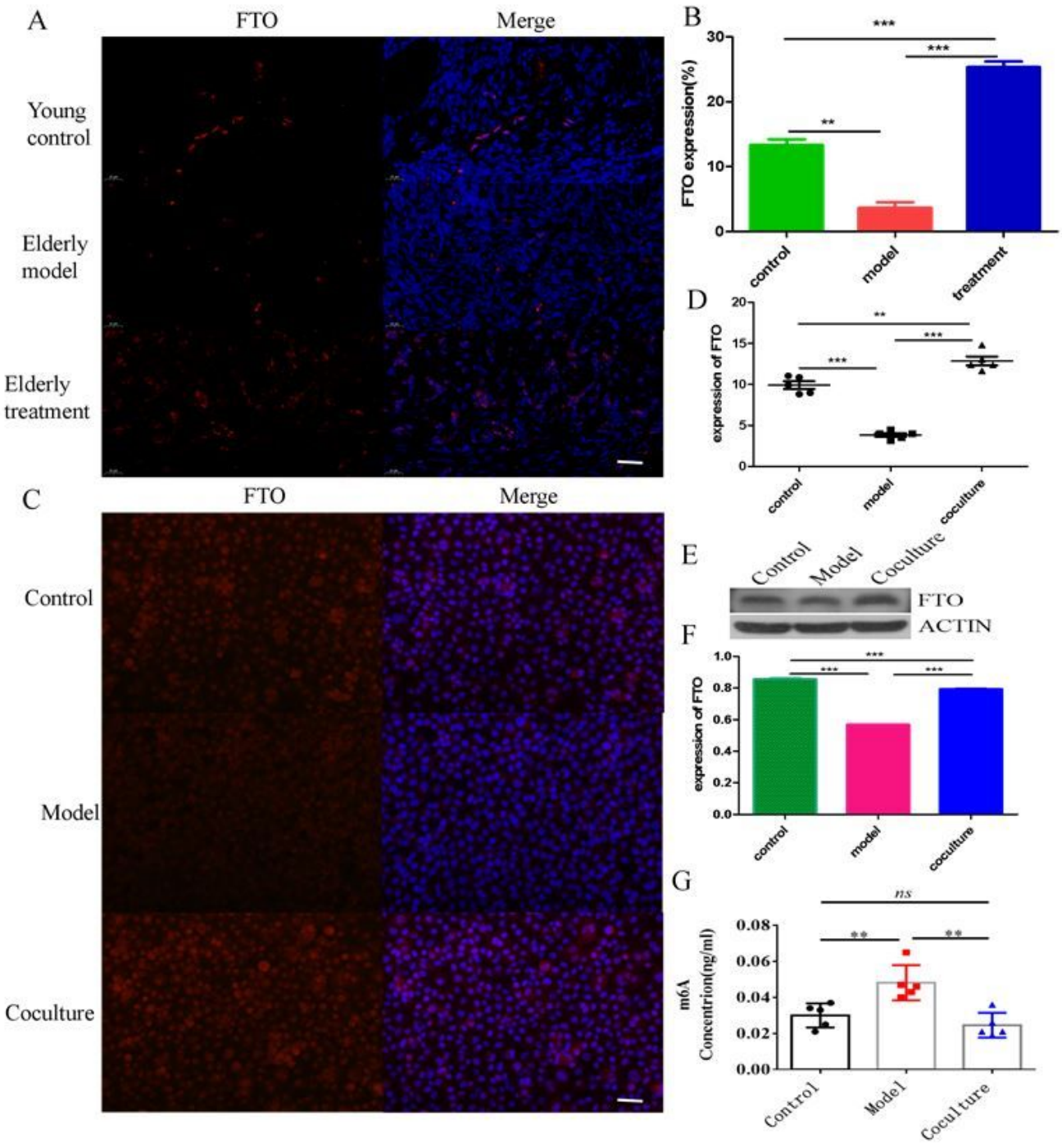

Figure 2

The changes of m6A methylation modification. **A-B** Immunofluorescence staining detected the expression of FTO in ovarian tissues(40 μm). **C-D** Immunofluorescence staining detected the expression of FTO in hGCs (400×). **D** the concentrion of m6A. **E-F** Western blot detected the expression of FTO in hGCs. **G** Colorimetric detected the overall level of m6A.

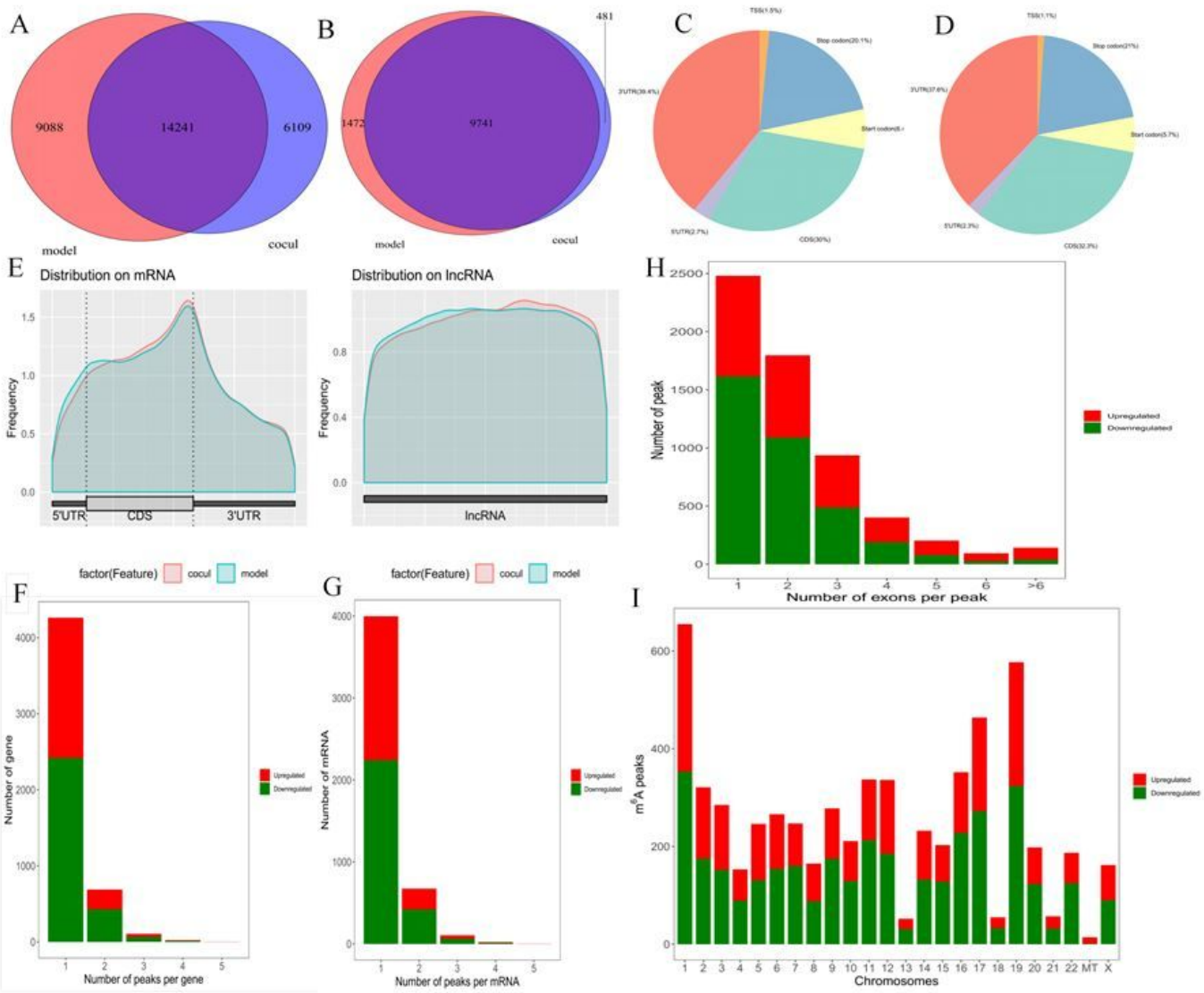

Figure 3

Overview of the m6A methylation landscape. **A** Venn diagram showing the m6A peaks. **B** Venn diagram showing the m6A-modified genes. **C-D** Pie charts showing the distribution of m6A peaks in the model and coculture groups. **E** Distribution of m6A peaks in mRNA and lncRNA. **F** Distribution of altered m6A peaks per gene. **G** Distribution of altered m6A peaks per mRNA. **H** Distribution of altered m6A peaks per exons. **I** Distribution of altered m6A peaks in human chromosomes. Fold change ≥2 and $P < 0.05$.

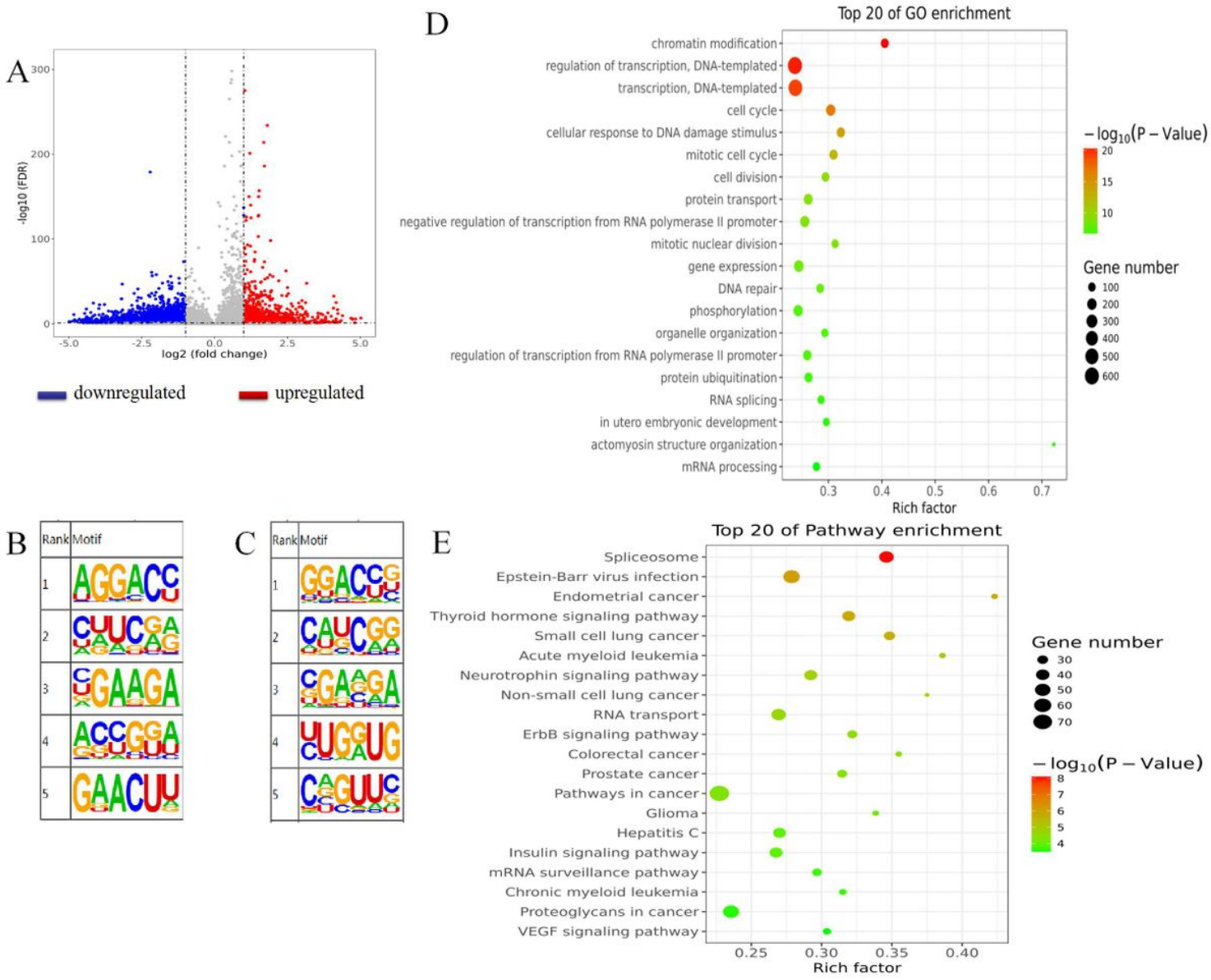

Figure 4

Biological significance analysis of differentially methylated RNAs. **A** Volcano plot showing the differential m6A peaks in the model and coculture groups. **B** the classic motif of model group. **C** the classic motif of cocolture group. **D** Bubble chart showing the top 20 enriched GO terms. **E** Bubble chart showing the top 20 enriched pathway terms.

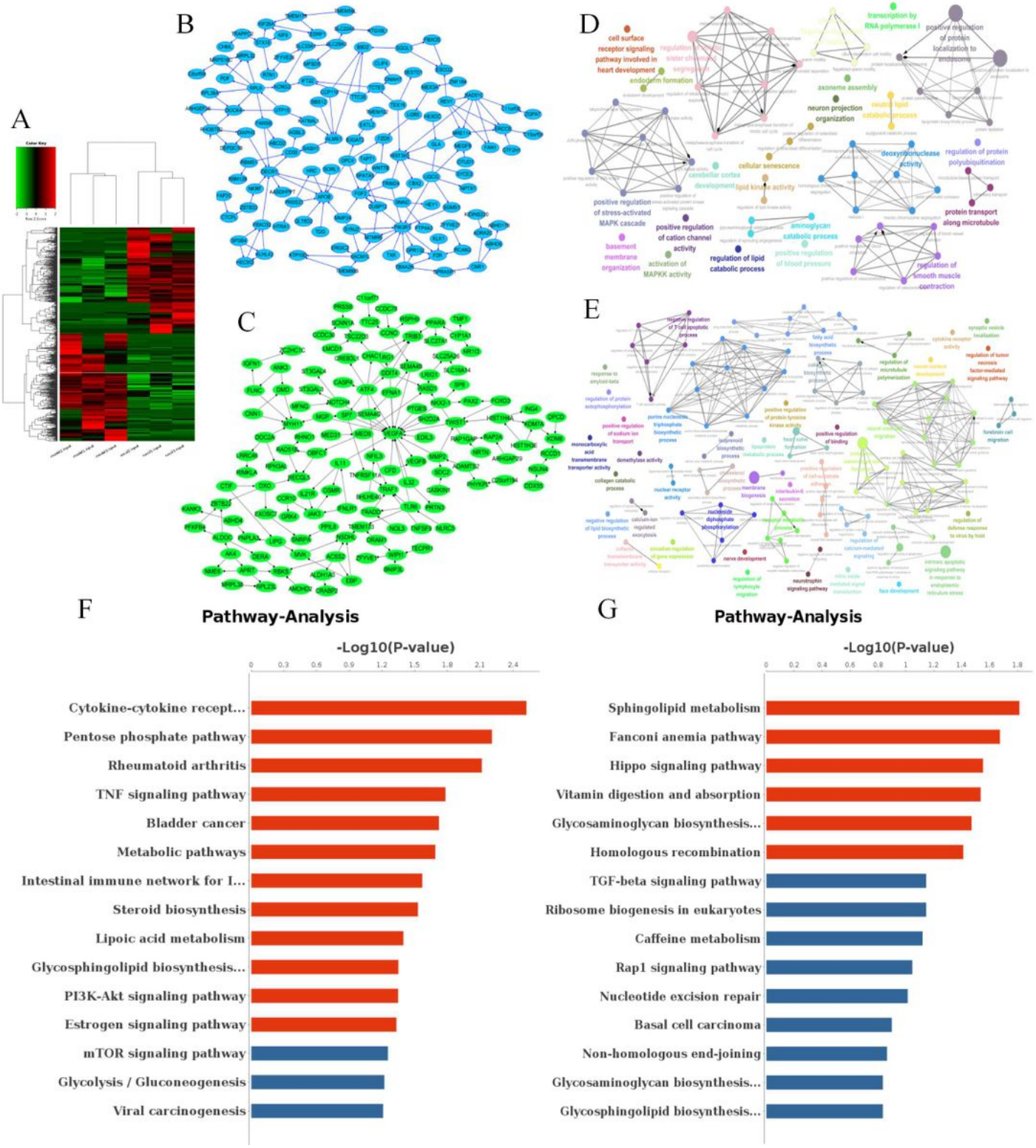

Figure 5

Analysis of the changes in transcriptome expression profile between the model and coculture groups. **A** Heat map showing the differential expression of RNAs in the model and coculture groups. **B** PPI networks of downregulated genes after cocultured with BMMSCs. **C** PPI networks of upregulated genes after cocultured with BMMSCs. **D** Functional interaction network of downregulated genes after cocultured with BMMSCs. **E** Functional interaction network ofdownregulated genes after cocultured with BMMSCs. **F** top

20 pathway terms of downregulated genes after cocultured with BMMSCs. **G** top 20 pathway terms of upregulated genes after cocultured with BMMSCs.

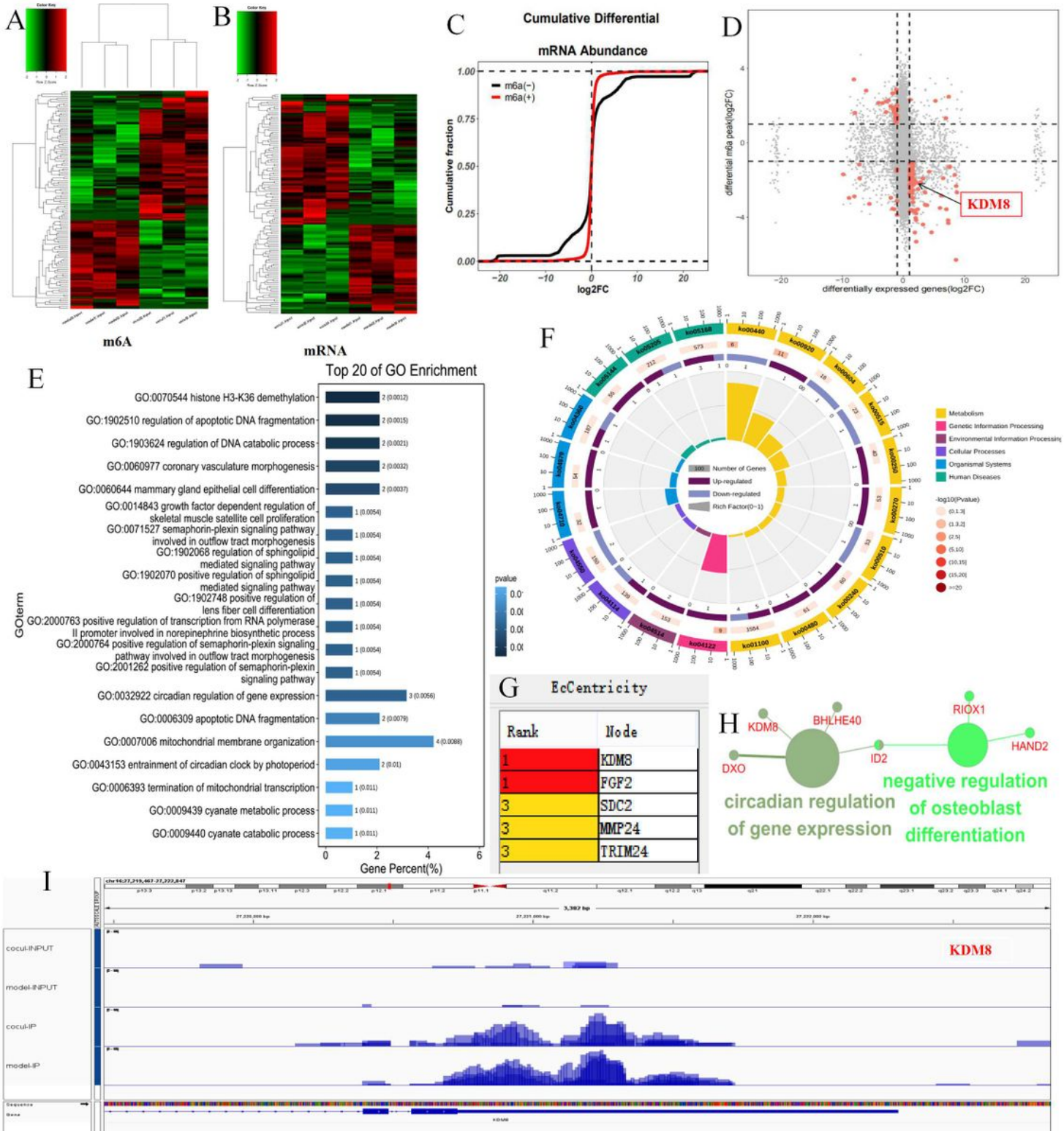

Figure 6

The correlation between differential m6A peaks and differentially expressed mRNAs. **A-B** Heat map of differential m6A peaks and differentially expressed mRNAs. **C** The cumulative differential mRNA

abundance. **D** Four-quadrant diagram showing correlations between m6A peaks and mRNAs. **E** Top 20 GO enrichment analysis results. **F** Top 20 KEGG pathway analysis results. **G** PPI network shows top 5 hub genes. **H** Pathway and functional enrichment of KDM8. **I** Visualization of KDM8 m6A peaks.

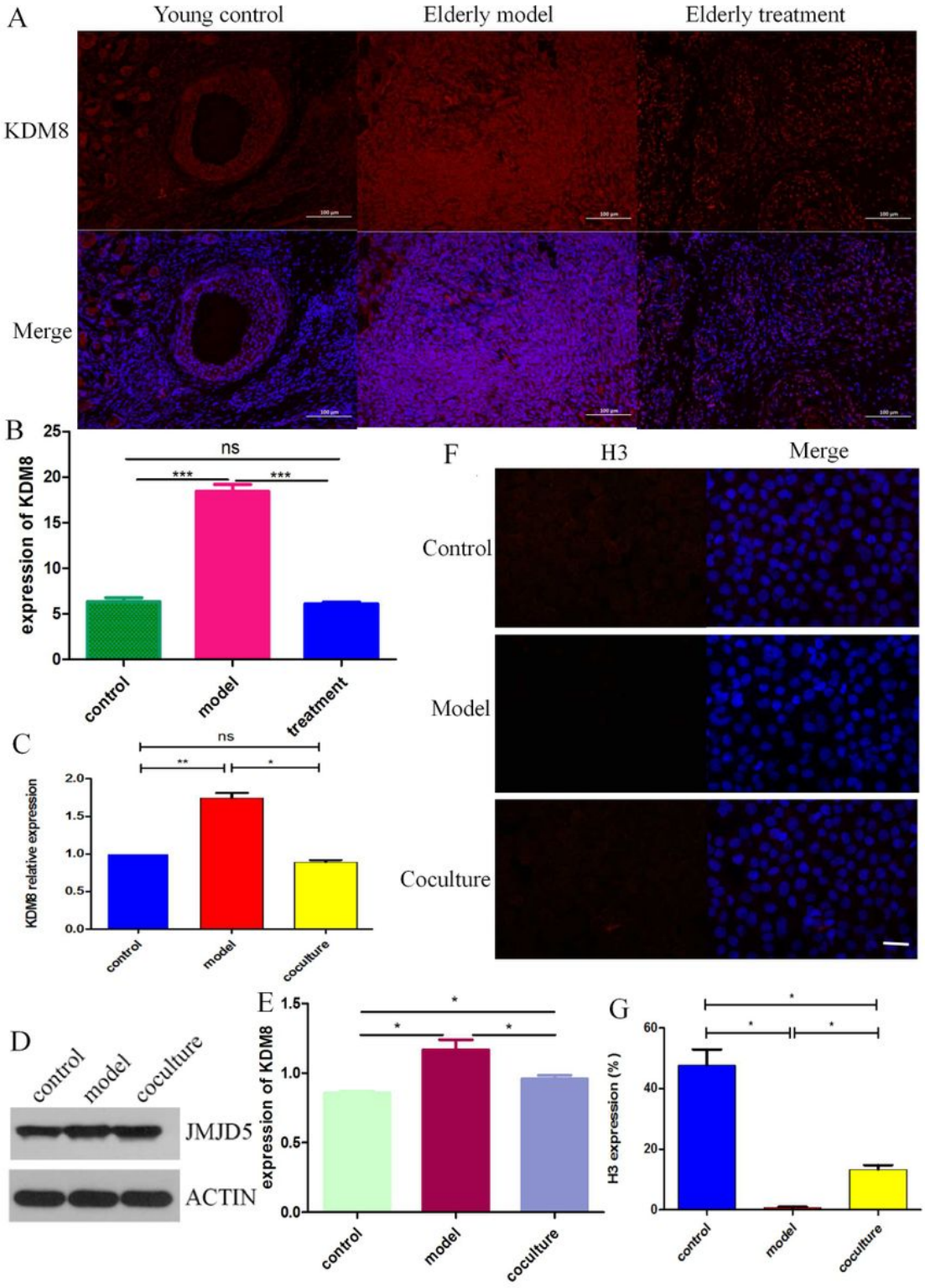

Figure 7

The changes of KDM8. **A-B** The expression of KDM8 in ovarian tissues of macaques. **C** The expression of KDM8 in GCs. **D-E** The expression of KDM8 in hGCs. **F-G** The expression of H3 in GCs.